A SYNTHETIC BIOACTIVE RESORBABLE GRAFT FOR PREDICTABLE IMPLANT RECONSTRUCTION: PART ONE

Maurice Valen
Scott D. Ganz, DMD

KEY WORDS

Synthetic
Resorbable
Bone graft
Bioactive
Bone regeneration
Chemotactic

Maurice Valen *is the president and director of research and development of Impladent Ltd; adjunct assistant professor, Department of Dental and Materials Science; and lecturer on restorative and prosthodontic sciences, New York University, College of Dentistry. Address correspondence to Mr Valen at Impladent Ltd, 198-45 Foothill Avenue, Holliswood, NY 11423.*

Scott D. Ganz, DMD, *is clinical attending at Hackensack University Medical Center, assistant clinical professor at University of Medicine and Dentistry of New Jersey, faculty and guest lecturer of numerous implant preceptorship programs nationally and internationally, and maintains a private maxillofacial prosthodontic specialty practice at 158 Linwood Plaza, Suite 204, Fort Lee, NJ 07024.*

Animal studies were conducted to evaluate the cell response and chemical potentiality of a synthetic bioactive resorbable graft (SBRG) made of nonceramic cluster particulate of low-temperature HA material. The study evaluated bone-bridging of the SBRG particulates in 1-mm wide implant channels of 5 × 8 mm long roughened titanium interface in 6 dogs and compared results to the same implant channels left empty as controls at 6- and 12-week intervals. Resorption rate capacity and cell response were evaluated with an assessment of the chemical characterization of the synthetic nonceramic material next to the titanium implant interfaces. Results of the animal studies were compared with human histologic biopsies of the SBRG for bone quality, density, and bone growth into defect sites concurrent with resorption time of the graft. One human biopsy consisted of a graft mixture of the SBRG and dense bovine-derived HA, compared under the electron microscope, including histology by H and E staining. Part 1 of this paper presents evidence of the predictability and efficacy of the SBRG osteoconductive, particulate chemical potentiality to aid in the regeneration of lost bone anatomy next to titanium implant interfaces. Recent technological innovations in computer hardware and software have given clinicians the tools to determine 3-dimensional quality and density of bone, including anatomical discrepancies, which can aid in the diagnosis and treatment planning for grafting procedures. When teeth are extracted, the surrounding bone and soft tissue are challenged as a result of the natural resorptive process. The diminished structural foundation for prosthetic reconstruction, with or without implants, can be compromised. A synthetic bioactive resorbable graft material having osteoconductive biochemical and biomechanical qualities similar to the host bone provides the means to improve compromised bone topography for ridge preservation, ridge augmentation, or to enhance the bony site for implant placement and subsequent prosthetic rehabilitation. Part two of this paper will demonstrate clinical applications of the SBRG material for purposes of implant placement and prosthetic reconstruction.

INTRODUCTION

Bone grafting has become a valuable mainstream clinical procedure, regardless of whether it is manufactured from organic or synthetic sources, which can be utilized in a variety of applications. Ridge preservation after tooth extraction can be important to preserve edentulous areas for later denture support, fixed bridge applications, implant reconstruction, and therapeutic maintenance of facial morphology by osseous reconstruction. Onlay grafts and combination bone grafts for sinus augmentation and periodontal procedures by the use of a synthetic bioactive resorbable grafts (SBRG) have become more predictable as treatment alternatives to restore form and function.[1–3] A variety of organically derived and synthetic dense bone formulations have been experimentally used as mixtures for the therapeutic repair and restoration of osseous ridge defect sites, post-tooth extraction (including periodontal reconstruction), sinus augmentation with implants, and cyst removals with questionable results.[4–6] Various resorbable and nonresorbable materials have been developed to provide clinicians with bone substitutes that can be used to enhance new bone formation next to the titanium implant interface. Resorbable materials have been the product of choice for new bone growth followed by implant placement because of the materials that have chemical and mechanical properties similar to bone.[7–9]

Although autogenous bone grafts may be considered the optimal choice for augmentation, the procedure usually requires harvesting bone from a distant donor site and can be self-limiting with associated risks of complications to the patient and required restoration of the remaining defect site.[10–14] Demineralized freeze-dried bone allograft (DFDBA) or frozen bone from human cadavers as an alternative source raises concerns because of the possible inconsistency of results and the possibility of donor sources transmitting infectious diseases.[15] Results of clinical and histologic studies suggest that DFDBA used today may have little or no osteoinductive/conductive capacity.[16] In a related study, Becker et al[17] concluded that not only does DFDBA not induce bone formation, but most importantly, it will not resorb, maintaining a spongy consistency that will interfere with ossification processes and act as an inhibitor to mineralization.

Patient aversion to human necrotic tissue graft and the risk of being subjected to possible viral infection from HIV donors is justified. As has documented, cases of disease transmission from osseous tissue by a seronegative donor have occurred.[18] The Federal Register published letters from the U.S. Food and Drug Administration that addressed the transmission of highly infectious diseases by warning that ''available scientific information indicated that these agents (bovine spongiform encephalopathy [BSE]) are extremely resistant to inactivation by normal disinfection or sterilization procedures.''[19–21] Although naturally derived materials, either human or bovine, are treated with gamma radiation, the possibility of disease transmission remains and must be seriously considered. The nature of organic material and the processing procedures of high heat or radiation may cause these materials to crystallize and harbor endotoxins or dormant pathogens.[18,22]

Ceramics, bovine, glass, and ceramic HA particulate materials merely act as filler materials because of their sintering density at high temperatures. These materials are subcategorized as nonresorbable, which can produce clinical complications such as fibrous tissue encapsulation, especially when used next to metallic dental implants.[23–25] Animal and human studies have concluded that ''nonresorbable'' materials act as barriers to bone-forming cells and behave as irritants because of their chemical and mechanical densities, which result in exfoliation, fragmentation, and the migration of such particulates to other organs. Fragmentation of these materials and the transport by giant cells of such dense particulates can settle in regional lymph nodes, lungs, and the spleen, resulting in the functional interference of these organs with systemic complications.[26,27]

To avoid biologic, systemic, and disease transmission complications, a nonautogenous bone graft material should ideally be nonantigenic, bioactive, osteoconductive, and synthetically derived with a clinically acceptable time frame of resorption by the majority of such material (ie, 6 months). Such material should have chemical and mechanical properties relatively similar to the host trabecular bone and possess a bioactive resorptive chemical potentiality to induce favorable cellular response for new bone formation by the action of ionization into calcium and phosphate ions in a chemotactic state.

A nonceramic bioactive bone augmentation material that meets these specifications has been commercially available for the past 15 years. It is provided as a sterile, biocompatible, and highly osteoconductive resorbable material with safer and more effective clinical results. This bioactive material of low-temperature HA cluster particulate (OsteoGen, Impladent Ltd, Holliswood, NY) mimics the structural configuration of bone trabeculation in a cluster-type format.

In numerous clinical and animal studies, when compared to various alloplastic materials, the resorbable low-temperature SBRG has been shown to produce better clinical results than surgical debridement alone or defects filled with dense particulate materials.[28–31]

In a review of the literature, the greatest success and biocompatibility of alloplastics was obtained with a low-temperature, synthetic, bioactive, calcium phosphate, resorbable material having a highly osteoconductive chemical potential. As the majority of re-

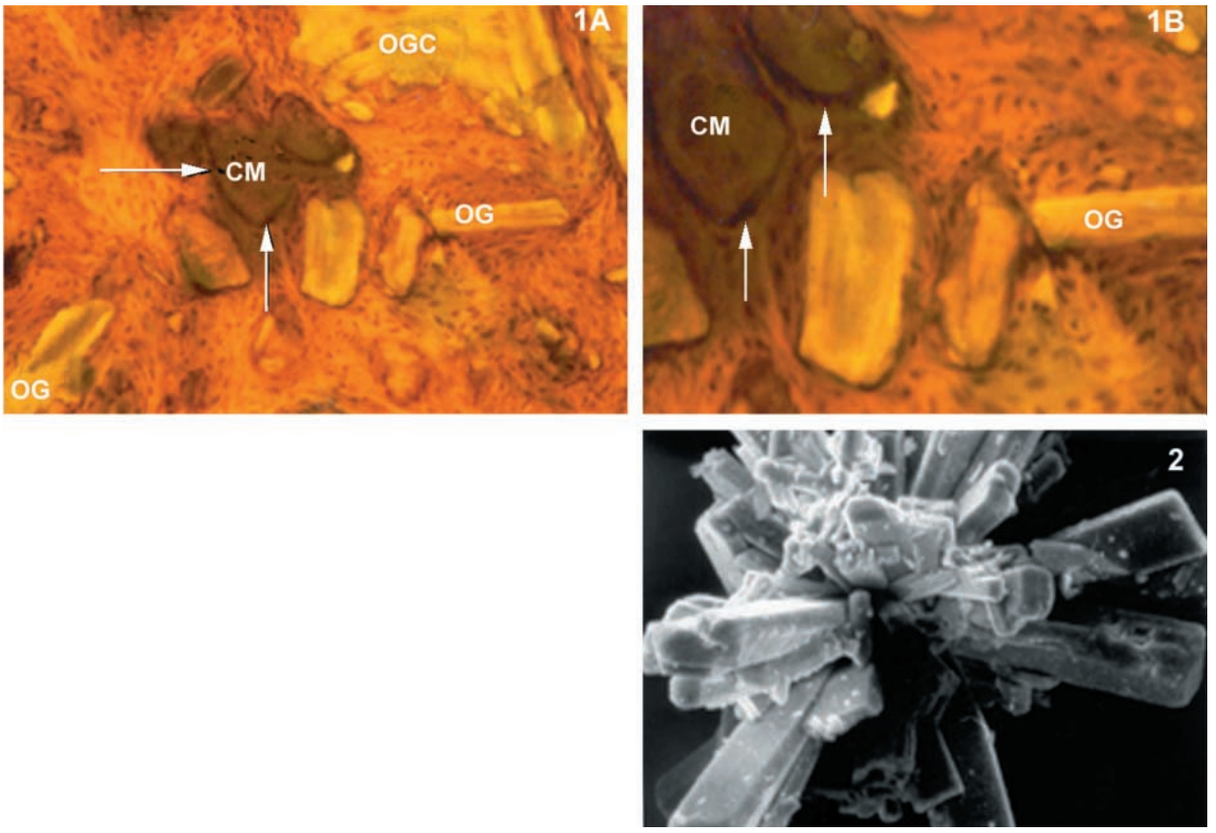

FIGURES 1 AND 2. FIGURE 1. (A) Human histology at 6 months shows mature bone formation into defect site concurrent with replacement of the synthetic bioactive resorbable graft (SBRG). Larger crystals (OG) or clusters (OGC) take longer to resorb without any fibrous tissue formation. Conversely, the HA ceramic material was fibro-encapsulated (arrows) and surrounded by macrophages and multinucleated giant cells noted as greenish gray areas over the ceramic material. (B) Closeup of fibro-encapsulated ceramic materials. FIGURE 2. Scanning electron micrograph of the SBRG bone augmentation materials showing 1 cluster of resorbable low-temperature crystal particulate attached to a center-like nucleus. This crystal morphology has similar chemical and mechanical properties as trabecular bone and provides a high state of hydrophilic response when the material is compacted into an osseous defect. The composite acts as a trellis mechanism for bone bridging in a chemotactic state by controlled resorption resulting in new bone formation.

sorption occurs between 4, 6, or 8 months postoperatively (depending on material quantity delivered, patient metabolic state, and vascularity), 80% of the material resorbs and the restored site is radio-opaque, demonstrating a state of high mineralization and bone densification.[32–35]

A 3.5-year clinical study using SBRG in conjunction with titanium implants for sinus elevation followed with histologic observation showed dense mineralization.[36] However, close examination of the histologic slide revealed the use of ceramic materials followed by their migration and fibrous tissue encapsulation (Figure 1A and B). The ceramic material was placed as an overlay graft to add bulk to the ridge and to "enhance pontic adaptation and help prevent tissue invagination."[37] It bears noting that material migration of the ceramic material did occur from the superior area of the implant ridge downward to the defect site, followed by material fragmentation and transport to regional organs.[26,27]

MATERIALS AND METHODS

The physiologic response of OsteoGen, an SBRG of low-temperature HA, was investigated in an animal model by packing (grouting) the material in titanium implant channels measuring 5 × 8 × 1 mm apart, which were subsequently implanted in the lateral distal femur of 6 dogs. Our study evaluated the bioactive, osteoconductive resorption rate, bone bridging, and cell response of the SBRG next to the titanium implant interface. Three dogs each were sacrificed at 6 and 12 weeks postoperatively. Undecalcified specimens were fixed in acrylic blocks for light microscopy and microradiography and stained using Masson, von Kossa, or trichrome techniques. Six titanium chambers consisting of 40 implant channels were evaluated: 20 channels as controls and 20 as experiments with this crystal cluster particulate material. Controls were filled with intramedullary blood opposing the titanium implant interface. The experimental channels were hand-packed with a slurry of 5 ml of blood and 3 g of sterile SBRG. The study examined

the materials' resorptive capacity, osteoconductivity for bone bridging next to a titanium implant, chemotactic potentiality to induce cell response for new bone formation, and the process of ionization or resorption by a bioactive device. Crystal morphology, density, and chemical composition of the material provided the key mechanism for controlled resorption in situ. Structurally, the particulate mimics the spicules of bone trabeculation by its cluster-like format, providing a trellis mechanism for hydrophilic and bioactive response for cell attraction through the process of progressive resorption and chemical attraction (Figure 2). The crystal-size distribution of the clusters enhances bulk density for an ideal time resorption mechanism of this bone augmentation material. Individual clusters may reach a maximum size of 600 μm. Due to its low aqueous buoyancy, the material must be packed in defect sites very aggressively for better osseous restoration by controlling excessive bleeding and empty spaces.

The proprietary manufacturing process is by a low-temperature precipitation/hydrolysis mechanism in a controlled environment for crystal growth and maturation. The SBRG is not sintered like ceramic HA. By avoiding high temperatures, the material does not lose its natural state of the HA synthetic bone composition and crystal morphology for $Ca_{10}(PO_4)_6(OH)_2$. It is not converted to tricalcium phosphate $Ca_3(PO_4)_2$ (TCP) by heat or tetracalcium phosphate $Co_4(PO_4)_2O$, (TetCP) and will not convert to an oxyapatite $Ca_{10}(PO_4)_6O_2$ (dehydroxylation) as do ceramic HA materials having secondary phases of α/β TCP, which make them biphasic, as well as pyrophosphates acting as bone inhibitors.[38,39] Infrared spectroscopy of the SBRG was performed with a Perkin-Elmer model 1430 and compared with mammalian bone on record, including X-ray diffraction of ceramic HA.

RESULTS

Infrared spectroscopy of the SBRG material clearly revealed the presence of the OH absorption as shoulders at 630 and 3570 cm^{-1}, which indicates high crystallinity by large structured crystals common to the hydroxyl group, with CO_3^{-2} (carbonate ions) content at 1450 cm^{-1} indicative of human bone minerals (Figure 3A).

By contrast, infrared spectroscopy of ceramic HA revealed the absence of OH and CO_3^{-2}, which classifies that material as an oxyapatite.[40] The splitting of the phosphorus-oxygen bending mode is a measure of higher crystallinity, size, and perfection. In SBRG and biologic apatites, the band is identified by higher splitting at 550 to 600 cm^{-1}, indicative of higher crystallinity and crystal maturation. A high-temperature ceramic HA shows that the crystal structure is distorted or destroyed by the heating process (Figure 3B). This results in a crystal structure that is not like biologic apatite or SBRG and will not resorb within an acceptable and effective clinical time–related benefit. SBRG is chemically and crystallographically similar to human bone mineral and is not related to high-temperature ceramic HA.

A cross-reference to X-ray diffraction analysis for HA, as per American Society for Testing and Materials powder diffraction protocol 9-432, confirmed the infrared analysis indicating that no phases other than crystalline HA were present for SBRG. X-ray characterization of the SBRG has identified 2 minor constituents to be crystalline phases of the brushite/monetite category. Animal studies by Urist and Dowell[41] and others[41–43] have identified the chemical potentiality of brushite/monetite or variations thereof, which may include octacalcium phosphate, to be a precursor and a seeding mechanism in the first stage of bone mineralization in an embryonic environment.[42–44]

Histologically, the blood in all 20 commercially pure titanium implants of the control channels were completely replaced by loose fibrous connective tissue at both time periods. These channels had small amounts of newly formed bone (only 1 mm) that extended into the channels on either end. Some osteoblasts were seen in the network of thin trabecular woven bone formation. A 75 to 100 μm layer of fibrous tissue was seen separating the titanium interface from the woven bone. By the 12th week, the tissue at some areas was as much as a 200 μm layer of connective tissue seen separating the commercially pure titanium interface. Osteoid was seen on less of the trabecular surfaces than in earlier time periods. Both bone and soft tissue exhibited more mature characteristics at 12 weeks than at 6 weeks. By the 12th week, the trabeculae had progressed further in less than half of the channels. The remaining connective tissue had matured, becoming less cellular and more organized (Figure 4A).

The presence of the SBRG low-temperature, osteoconductive, resorbable bone augmentation materials within the channels significantly enhanced the ingrowth of bone through and up against the commercially pure titanium with little or no fibrous tissue 1 or 2 layers thick between the bone and the commercially pure titanium interface (Figure 4B).

Microradiographic comparison of individual crystals next to the ingrowth of bone showed extensive bone attachment to the SBRG crystals and bone maturation in the process of osteon-like formation. Some haversian canals are seen as black holes, which represent marrow cavities becoming narrower in size over time. This continuous bone maturation inside the haversian canals represents the continuous bone buildup in a circumferential layering fashion through the osteoblastic synthesis by the cells (Figure 5).

Scanning electron micrograph analysis of a fractured crystal specimen at 6 weeks showed evidence of direct bone trabeculation attachment to the SBRG crystal particulates. This crystal sample shows cell proliferation and attachment with high binding capacity to their surfaces. Crystallographically, the fractured crystal can be identified by its small parallel crystallite structure

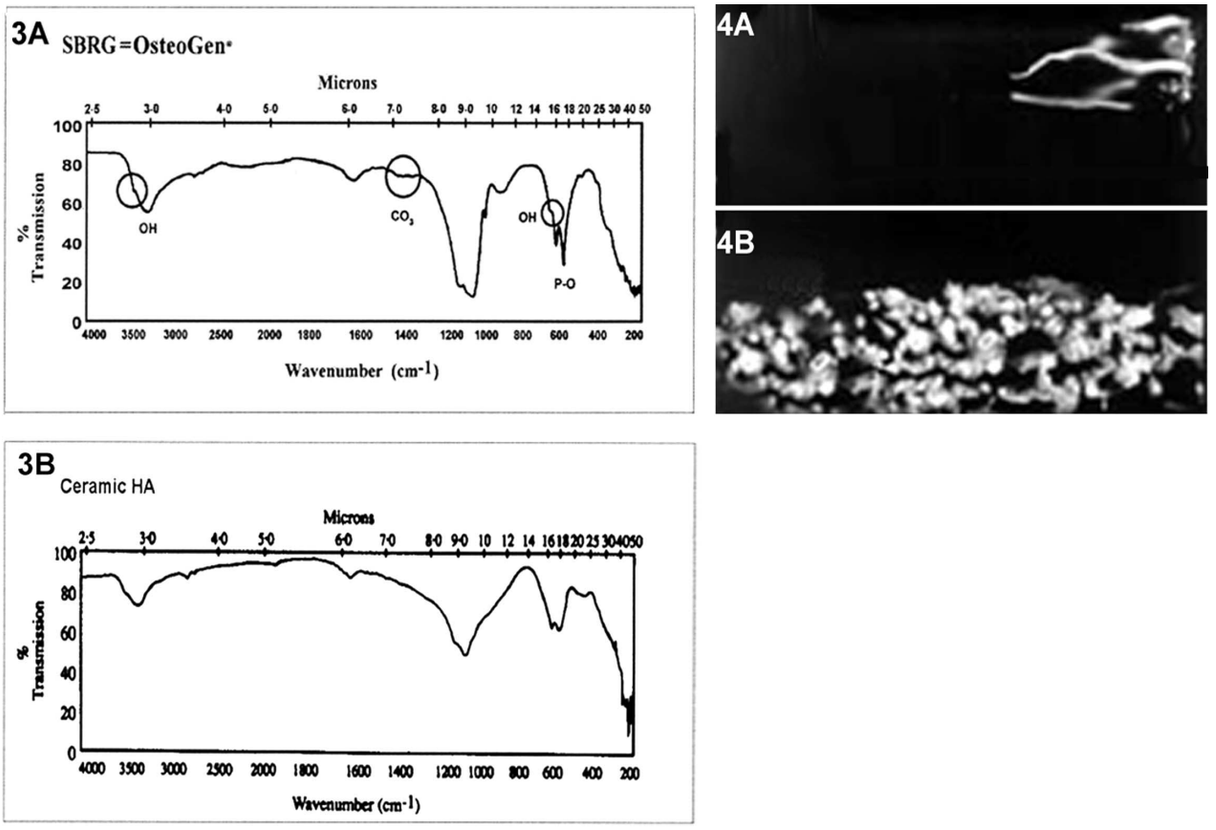

FIGURES 3 AND 4. FIGURE 3. (A) Infrared spectroscopy of the synthetic bioactive resorbable graft (SBRG). Note the OH bands marked by the circles as peaks at 630 and 3510 cm^{-1} and a peak at 1450 cm^{-1} for the CO_3 (carbonate) group, indicating higher crystallinity than biologic HA, but with overall similarity to the biological mineral. A comparison of the infrared spectra of OsteoGen and ceramic HA shows considerable differences between them, which is indicative of the high-temperature treatment of the ceramic material that makes the ceramic very different than the SBRG. It is these differences that make SBRG resorbable and ceramic nonresorbable. (B) Infrared of ceramic HA is quite different from that of SBRG. Note the absence of OH and CO_3 bands. The broadening of peaks at 750 to 1450 cm^{-1} are indicative of dense materials (ie, ceramic, bovine, etc.). This broadening indicates distortions in the crystal lattice due to high-temperature processing and chemical conversion to oxyapatite (not a true HA product). FIGURE 4. (A) Microradiograph of titanium implant vent without the low-temperature SBRG at 6 weeks. Minimal bone osseointegration is noted by thin trabeculae having been preceded by a connective tissue inhibiting osseous bridging. (B) Implant vent that was packed with low-temperature SBRG exhibited crystal resorption concurrent with bone bridging 8 mm across at 6 weeks.

having an uniaxial laminated arrangement. The crystals are identifiable by their tetragonal or hexagonal shape, having ultrastructural architecture similar to biologic HA. This uniaxial laminate crystallite arrangement, in the order of 500 to 1000 Å, is ideal for cell mediation and resorption by hydrolysis (Figure 6; see arrow). In contrast, ceramic HA, glass, plastic, and bovine bone are monolithic, and some are very dense. Their relationship to cellular activity is by fibro-encapsulation, especially under load. In comparison to the size of the monolithic-dense particulates, the macrophages and giant cells are too small and the cells will fragment the dense particulates and transport these materials to the regional lymph nodes, lungs, and spleen for further processing, interfering with the normal function of such organs.[26,27]

The primary characteristic of the osteoblast cell is the mineralization caused by the laying down of a procollagen matrix as the foundation for new bone formation. The 12-week specimens and radiographic examinations of the implant chambers filled with SBRG showed complete filling of all channels with new bone. The trabeculae had progressed further than the 6-week specimens and had thickened and bridged through the channels, exhibiting lamellar remodeling (von Kossa stain) (Figure 7). At 6 weeks, the ingrowth of bone was seen to be a vascular woven bone with thin trabeculae, including osteoid tissue (red area) and numerous osteoblasts in the process of new bone formation in a lamellar fashion. In some areas of the bone, it had thickened to form circumferential structures of osteons. The ingrown bone was shown to surround the remaining SBRG crystals and formed a direct bond attachment to the particles without any visible interposing tissue (Masson stain) (Figure 8).

A photomicrograph of the 12-week SBRG specimen next to the titanium

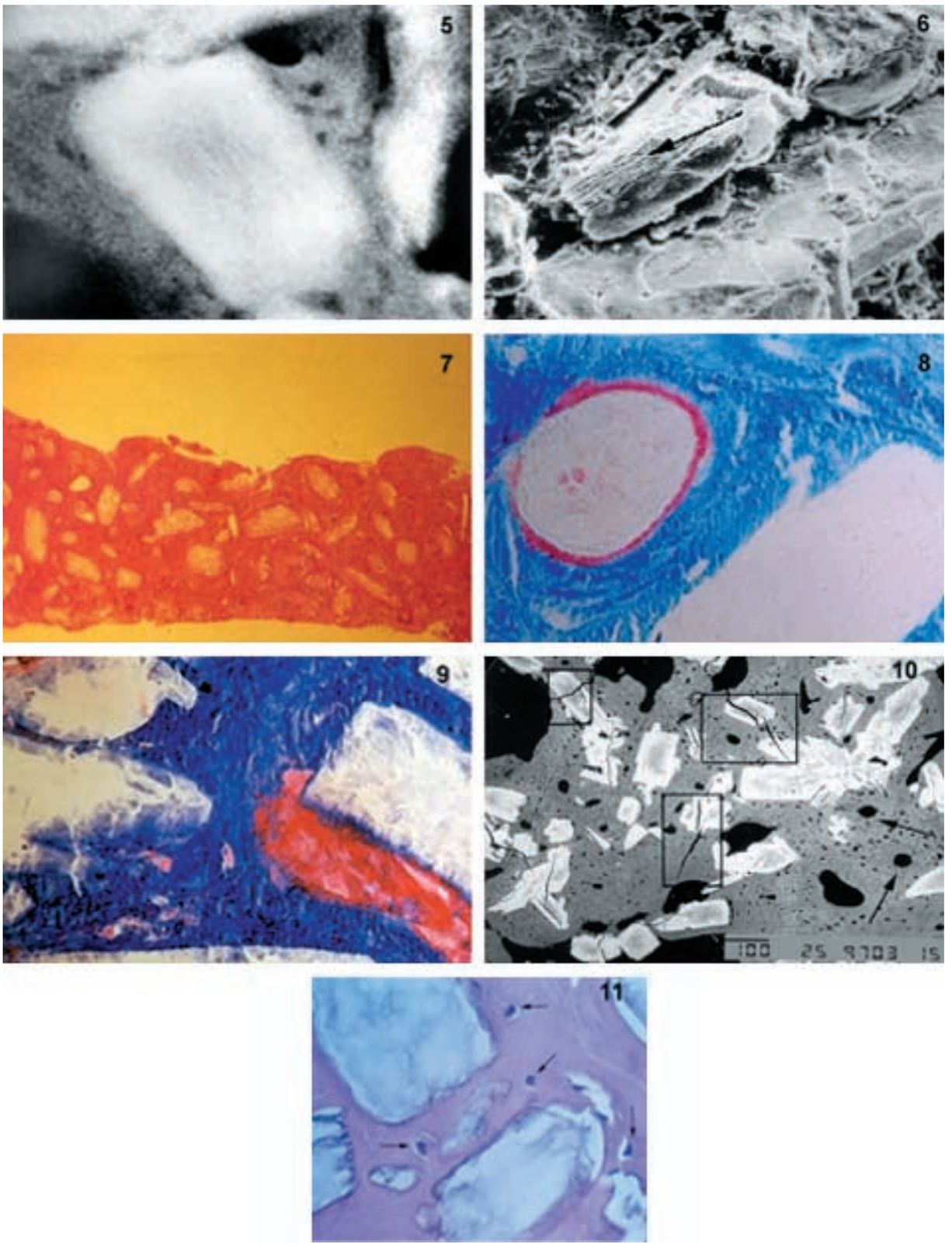

implant interface showed mature bone formation (Figure 9, dark blue area). The few remaining larger crystals showed surface pitting with rounded corners, denoting a time-related controlled resorption mechanism by a denser and larger crystal. The red area shows the presence of osteoblast cells. At their dormant state, the cytoplasm of the osteoblast cell stain light pink. When the cells are red or darker, they are at their active state, exhibiting active bone mineralization indicated by their cytoplasmic basophilic response (dark red or light purple; Figures 8 and 9). In comparison to the 6-week histologic slide (Figure 8), note the darker blue color characteristic of well organized and denser bone. Developing osteons are seen at different stages of remodeling and are formed by the progressive and continuous buildup of concentric bony lamellae (Figure 10). Their haversian canals (small black circles) of marrow-filled cavities narrows in size through the osteoblastic synthesis of new bone formation. This process will be followed by osteoclastic activity and the subsequent enlargement of the haversian canals showing larger black circles. As this destruction ceases, the process of osteoblastic activity begins once more. This phenomena will be repeated 3 times within an approximate course of 142 days, depending on the metabolic activity of the host. One indication of the SBRG having similar mechanical properties to the host is the fracture line of bone traversing across the crystal structure without the particulates dislodging or fibro-encapsulating within the new osseous structure after loading (noted in the boxed areas of Figure 10). This benefit is indicative of synthetic materials having a similar modulus of elasticity to the host bone ideal for implant placement.

In the final process of bone formation and maturation, the osteoblast cell will be entrapped at its new residence in the bone matrix and is renamed an osteocyte. Osteocytes reside in lacunae, indicating that the process of bone maturation has been completed (Figure 11). In addition to these experiments, we present a clinical case that further illustrates the above-mentioned benefits relating to the in vivo use of the SBRG.

Case Study

A 32-year-old woman presented with a failing right posterior second molar and missing the first molar tooth. Using standard panoramic and periapical radiographs, assessments were made as to the bone height for placement of the endosseous root-form implants (Figure 12). Although not realized at the time of surgery because of the limited diagnostic capacity of the panoramic radiograph, there was an area of poor bone quality between the buccal and lingual cortical plates (Figure 13). However, the mesially tilted second molar was extracted, and a press-fit cylinder implant was placed anteriorly without incident.

An osteotomy was prepared to place an implant distal to the second premolar tooth. Using the recommended technique, an implant was delivered to the site. Upon releasing the implant from the carrier, and rotating the implant into the osteotomy site, it abruptly dropped into a large cavity in the mandible. The lack of medullar bone between the cortical plates was not detected with conventional radiographs, yet it was a clinical reality. A periapical radiograph was taken immediately. The radiograph revealed the implant lying horizontally near or on top of the mandibular canal (Figure 14). Once located, the task of retrieving the implant proved to be a difficult one. In order to visualize the implant and gain proper access, the first fixture placed distally was removed. Under magnification for better visualization, the implant was ''backed out'' of the original implant's osteotomy, apical end first.

Immediately after the implant was retrieved, the internal cavity was debrided using hand instruments and

←

FIGURES 5–11. FIGURE 5. Microradiograph at 6 weeks of bone ingrowth into the implant channel. Bone is in direct contact with the synthetic bioactive resorbable graft (SBRG) crystal cluster particulate (arrow). The resorbing crystals are incorporated and directly bonded into the new bone without any intervening fibrous tissue present or any mechanical or chemical challenge due to similar properties to the host bone. FIGURE 6. Scanning electron micrograph analysis of a fractured crystal showing a cross-section of laminated crystallites parallel to each other (arrow). Morphologically, such arrangement provides strength. Hydrolysis provides ability for cell proliferation and controlled resorption to ionize in situ into calcium and phosphate ions. FIGURE 7. Scanning electron micrograph of 12-week dog specimen. On average, 70% to 80% of defect site has been filled with well-organized mature bone formation. Some larger crystals/crystal clusters take longer to resorb, and their resorption is dependent on cellular physiologic equilibrium for osseous restoration. The SBRG-remaining particles are in direct new bone apposition and incorporated into newly formed bone showing no intervening soft tissue or any inflammation. FIGURE 8. Photomicrograph of implant channel filled with SBRG at 6 weeks, showing enhanced bone ingrowth. Light blue represents new bone formation. White rectangle shows the SBRG space occupied previously by the crystal structure. The red circle with its center (Haversian canal) demonstrates the beginning of new bone matrix (osteoid). Calcium phosphate is then added to the matrix in a circumferential pattern to form new bone (osteon formation); this process requires the presence of osteoblasts (red area; Masson stain). FIGURE 9. Photomicrograph specimen at 12 weeks. The darker blue area shows well-matured bone formation within the defect site having limited marrow spaces. White areas are of larger SBRG crystals in the process of resorption. Smaller crystals would have resorbed at 4 to 6 weeks. The red area shows active osteoblast cells as noted by their cytoplasmic color change (basophilic). FIGURE 10. Haversian canals are noted as black holes (arrows) having a well-organized concentric bone formation. Fracture lines of bone traversing across the crystal structure after loading is indicative of materials having a similar modulus of elasticity (shown in boxed areas). FIGURE 11. Human biopsy of case study at 6 months. Hematoxylin and eosin-stained photomicrograph showing well-organized new bone formation to SBRG crystals without intervening soft tissue. Note osteocytes within the lacunae (arrows) denoting mature bone formation. Concentric layering of lamellae are noted at the upper right corner.

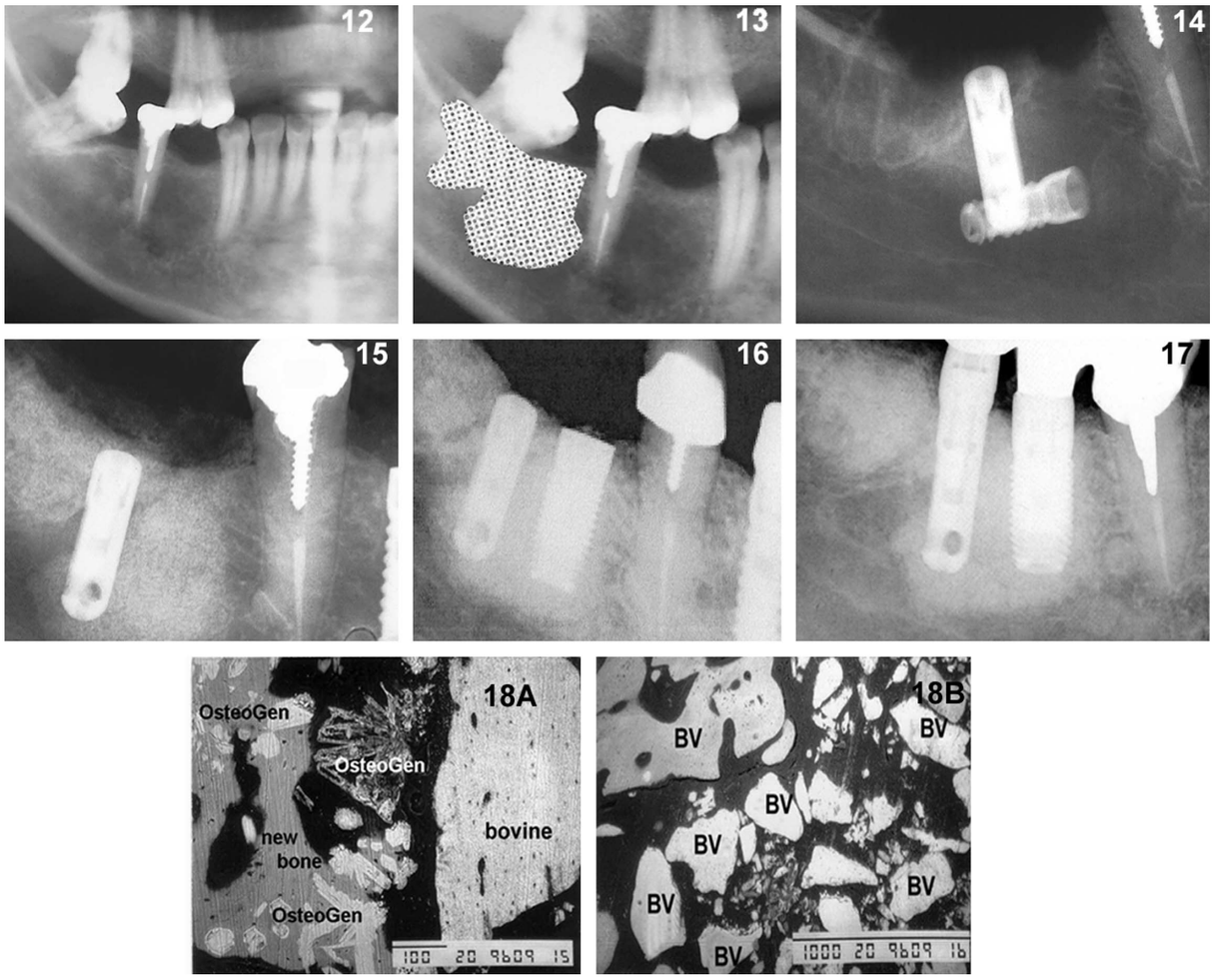

FIGURES 12–18. FIGURE 12. Preoperative panoramic radiograph. FIGURE 13. Area of poor bone quality is indicated by textured overlay. FIGURE 14. Second implant lost in hollow bone area. FIGURE 15. Immediate postoperative radiograph showing radiopaque area of ceramic bovine bone graft material placed in mandibular cavity. FIGURE 16. Wider 4.7 mm diameter implant in previously grafted site. FIGURE 17. Radiograph of site after 40 months in function. Note apparent density in the area of interest. FIGURE 18. (A) Backscattered electron imaging of human biopsy at 4 months showing new bone formation concurrent with crystal resorption of the SBRG. Larger crystals are encased within new bone formation without tissue encapsulation. Ceramic bovine particulate shows only fibrous tissue encapsulation. (B) This specimen consists mostly of bovine particulate with fibrous tissue encapsulation.

round burs with irrigation. A combination of radiopaque (ceramic) bovine OsteoGraf 300 (CeraMed, Denver, Colo) and OsteoGen (a radiolucent synthetic, bioactive, resorbable graft) was delivered to the site and expressed through a wide syringe. The grafting composite was condensed thoroughly into the molar site of the large cavity (Figure 15). The first implant was then placed back into the original osteotomy. The tissues were approximated, and primary closure was achieved. Another implant was placed mesial to the second premolar without incident. The grafted site was allowed to heal for 4 months before re-entry.

After 4 months the site was reopened and an osteotomy was prepared into the newly grafted bone. The bone was found to be dense and well compacted. A wider (4.7-mm wide) screw-type implant was then placed into the grafted site (Figure 16). A core sample of the bone was taken for histologic examination, including a scanning electron micrograph analysis of the graft composite. The wide implant was allowed to integrate for 4 months prior to loading. All of the implants were then uncovered, and the restorative phase was completed. After 40 months in function, the SBRG radiolucent graft material had a radiopaque denser appearance with well-organized bone formation, and it exhibited no crestal bone loss (Figure 17). The molar area exhibited a similar appearance. Figure 18A and B shows backscattered electron imaging of the human biopsy consisting of SBRG and dense bovine particulates. The SBRG was manufactured at approximately 100°C, and the deorganified bovine particulate materials were sintered at

about 1150°C. Only the SBRG is associated with well-organized bone formation. The remaining crystals are surrounded by well-organized new bone formation concurrent with crystal resorption in such areas (Figure 18A). The bovine particulate shows only fibrous tissue encapsulation. In Figure 18B, the specimen consists mostly of bovine particulate encased in fibrous tissue with no visible bone formation. Such material is radio-opaque from the day of placement.

Discussion

The histologic observation from this and other studies relevant to human physiology is that, on the average, connective tissue may migrate on a titanium surface without SBRG as much as 0.5 mm a day, whereas bone may take 3 months to accomplish such a journey, especially if the surface is smooth. On a roughened titanium implant interface, cells will take longer to migrate because of the ''hurdling effect,'' although adhesion ability to a roughened surface is advantageous for implant stability. Roberts et al[45] concluded that following surgery the osseous interface adjacent to an implant can be classified as woven bone. Woven bone has a relatively low mineral content with randomly oriented fibers providing minimal support or strength at the implant interface. On a closer observation at the bone-tissue interface following surgery, Roberts[46] concluded that ''about 1 mm of compacta adjacent to the osseous wound undergoes necrosis postoperatively, despite optimal surgical technique.''

Brunski[47] reported that the bone-implant interface next to Branemark implants, following surgery, may have questionable stability because of the presence of large trabecular spaces, poorly mineralized bone, and high fat cell content. He concluded that the bone-implant interface of intimate contact is approximately 45% on average. It bears noting that the disadvantage of a ''very rough implant interface'' (ie, push-in implant or annular) is its initial percentage of intimate bone contact, the day of implant placement, which may be reduced as much as 50% by the implant's concavities or finlike design, whereas the minor diameter of the implant is not in contact with bone. Based on the present animal study such implant compromise can be altered into such implant undercuts by the use of an SBRG grouting technique. These crystals of similar chemical and especially mechanical properties as the host bone demonstrate an excellent adaptability as a grouting graft for large trabecular spaces and implant concavities. Meffert[23] and Zablotsky[24] pointed out in their studies that very dense material (i.e., ceramic HA or glass) next to implants and bone interface may present a greater challenge to the bone, resulting in unpredictable bone regeneration due to fibrous tissue.

This study has demonstrated that the use of the synthetic bioactive, osteoconductive SBRG was able to bridge bone across 8 mm into implant channels against commercially pure titanium in a symmetric fashion without any connective tissue as long as the site was overfilled and well compacted.

The presence of the low-temperature crystalline material, acting as an intermediate bone-filling substitute next to the titanium implant interface, was associated with a large increase of bone ingrowth. By contrast, unfilled titanium channels have an identical titanium interface filled with connective tissue. At both time intervals, the material showed signs of progressive dissolution and replacement by bone. The remaining SBRG material was firmly incorporated into new bone without any intervening spaces and did not act as a weak point to provide fracture initiation because of a similar elastic modulus as the host bone. SBRG clearly has a bioactive chemotactic response that promotes bone ingrowth into defects through bone attachment and conduction from particle to particle. It is observed by this and other studies that the chemical potentiality may act as a deterrent or minimize connective tissue migration into implant channels.[48] This is in significant contrast to other dense materials (ie, ceramic HA, glass, plastics, and bovine).

Conclusion

Part 1 of this 2-part series presented animal studies that were conducted to evaluate the osteoconductive potentiality of the SBRG, which is a nonceramic particulate of low-temperature HA material. This study, including a clinical case, evaluated bone-bridging of the SBRG in various restorations. Resorption-rate capacity and cell response were also evaluated, with an assessment of the chemical characterization of the material. Results of the animal studies were compared with human histologic biopsies of the commercial product for bone quality, density, and bone ingrowth into defect sites, especially next to titanium implants and its relationship to the host response. It was concluded that SBRG is ideal for implant placement, providing implant support and bone densification. Additionally, a composite graft mixture consisting of SBRG and mostly dense bovine-derived ceramic HA was compared under electron microscopy. The SBRG material has shown concurrent resorption, excellent bone regeneration, and densification about such crystal clusters without any compromise or adverse effect to implant interface or osseous environment. However, the dense bovine ceramic material (usually sintered above 1150°C) demonstrated fibrous tissue encapsulation about such dense particulates without any evidence of resorption or pitting of the particulate interface. Part 2 will demonstrate clinical applications of the bioactive resorbable material for purposes of implant placement and prosthetic reconstruction.

References

1. Vlassis JM, Hurzeler MB, Quinones CR. Sinus lift augmentation to facilitate placement of nonsubmerged implants: a clinical and histological re-

port. *Pract Periodon Aesth Dent.* 1993;5: 15–23.

2. Ganz SD. Mandibular tori as a source for onlay bone graft augmentation: a surgical procedure. *Pract Periodont Aesth Dent.* 1997;9:973–982.

3. Epstein SR, Valen M. An alternative treatment of the periodontal infrabony defect: a bioactive resorbable hydroxyl-apatite composite alloplastic graft. *J Periodontol.* In press.

4. Frame JW, Rout PG, Browne RM. Ridge augmentation using solid and porous HA with and without autogenous bone or plaster. *J Oral Maxillofacial Surg.* 1987;45:771–778.

5. Wallace SS. Histologic evaluation of sinus elevation procedure: a clinical report. *Int J Periodont Rest Dent.* 1996; 16:47–51.

6. Kwan JY, Meffert RM, Carr RF, Weir JC. Clinical and histologic evaluations of HTR alloplastic grafting material: case Report. *Int J Periodont Rest Dent.* 1990;10:293–299.

7. Smiler DG, Johnson PW, Lozada JL, et al. Sinus lift grafts and endosseous implants: treatment of the atrophic posterior maxilla. *Dent Clin N Amer.* 1992;36:151–186.

8. Whittaker JM, James RA, Lozada J, Cordova C, GaRey DJ. Histological response and clinical evaluation of herograft and allograft materials in the elevation of the maxillary sinus for the preparation of endosteal dental implants sites. Simultaneous sinus elevation and root form implantation: an eight-month autopsy report. *J Oral Implantol.* 1989;15:141–144.

9. Linkow LI, Wagner JR. Management of implant-related problems and infections. *J Oral Implantol.* 1993;29: 321–335.

10. Brazaitis MP, Mirvis SE, Greenberg J, Ord RA. Severe retro-peritoneal hemorrhage complicating anterior iliac bone graft acquisition. *J Oral Maxillofac Surg.* 1994;52:314–316.

11. Keller EE, van Roekel NB, Desjardins RP, Tolman DE. Prosthetic-surgical reconstruction of the severely resorbed maxilla with iliac crest bone grafting and tissue-integrated prostheses. *Int J Oral Maxillofac Implant* 1987;2: 155–165.

12. Catone GA, Reimer BL, McNeir D, Ray. Tibial autogenous cancellous bone as an alternative donor site in maxillofacial surgery: a preliminary report. *Int J Oral Maxillofac Surg.* 1992;50: 1258–1263.

13. Cain JR, Mitchell Dl, Markowitz NR, Wiebelt FJ. Prosthodontic restoration with dental implants and an intraoral cranial bone onlay graft: a case report. *Int J Oral Maxillofac Implant* 1993; 8:98–100.

14. Donovan MG, Dickerson NC, Hanson LJ, Gustafson RB. Maxillary and mandibular reconstruction using calvarial bone grafts and Brånemark implants: a preliminary report. *Int J Oral Maxillofacial Surg.* 1994;52:588–594.

15. Conrad E, Gretch DR, Obermeyer KR, et al. Transmission of the hepatitis-C virus by tissue transplantation. *J Bone Joint Surg.* 1995;77A:214–224.

16. Becker W, Urist M, Becker B, et al. Clinical and histologic observations of sites implanted with intraoral autologous bone grafts or allografts. 15 human case reports. *J Periodontal.* 1996;67: 1025–1037.

17. Becker W, Becker BE, Caffesse R. A comparison of demineralized freeze-dried bone and autologous bone to induce bone formation in human extraction sockets. *J Periodontal.* 1994;65:1128–1133.

18. Simonds RJ, Holmberg SD, Hurwitz RL, et al. Transmission of human immunodeficiency virus type 1 from a seronegative organ and tissue donor. *N Engl J Med.* 1992;726–732.

19. Henney JE. *Directive Addressed to Manufacturers of FDA-regulated Products.* Department of Health and Human Services; December 17, 1993;29:44591-4.

20. Friedman MA. *Directive Addressed to Manufacturers of FDA-regulated Drug/Biologic/Device Products.* Department of Health and Human Services; May 9, 1996;7:52345-b.

21. Kessler DA, *Directive Addressed to the FDA's Office of Health Affairs.* Department of Health and Human Services; August 29, 1994;7:52345-b.

22. Gross N, Dawley H, Carey J, Trinephi M, Miller KL. Mad cows and humans. *Bus Wk.* 22 December 1997;80–82.

23. Meffert RM. A bioactive ceramic glass material for the repair of periodontal defects. *Pract Periodont Aesth Dent.* 1996;8:1–6.

24. Zablotsky M. The surgical management of osseous defects associated with endosteal hydroxylapatite-coated and titanium dental implants. In: Sendax VI, ed. *Dental Clinics of North America—Hydroxylapatite Coated Implants.* Philadelphia: W.B. Saunders; 1992:117–149.

25. Froum SJ, Tarnow DP, Wallace SS, Rohrer MD, Cho SC. Sinus floor elevation using anorganic bovine bone matrix (OsteoGraf/N) with and without autogenous bone: a clinical, histologic, radiographic, and histomorphometric analysis—part 2 of an ongoing prospective study. *Int J Periodont Rest Dent.* 1998;18:529–543.

26. DiCarlo EF, Bullough PG. Biologic responses to orthopaedic implants and their wear debris. *Clin Mat.* 1992; 9:235–260.

27. El Sharkawy HM, Meffert, RM. *Biodegradation and Migration of Porous Calcium Phosphate Ceramics* [thesis]. New Orleans, La: Louisiana State University School of Dentistry; 1987.

28. Masters DH. Problem solving in implant dentistry. *J Am Dent Assoc.* 1990;121:355–358.

29. Corsair A. A clinical evaluation of resorbable hydroxylapatite for the repair of human intraosseous defects. *J Oral Implantol.* 1990;16:125–128.

30. Hurzeler MB, Quinones CR, Morrison EC, Caffesse RG. Treatment of peri-implantitis using guided bone regeneration and bone grafts, alone or in combination, in beagle dogs. Part II: histologic findings. *Int J Oral Maxillofac Implants.* 1997;12:168–175.

31. Hurzeler MB, Quinones CR, Morrison EC, Caffesse RG. Treatment of peri-implantitis using guided bone regeneration and bone grafts, alone or

in combination, in beagle dogs. Part I: clinical findings and histologic observations. *Int J Oral Maxillofac Implants.* 1995;10:474–484.

32. Ganz SD. Restoring the anterior maxillary arch with an implant supported fixed bridge. *Implant Soc.* 1993: 4:2–5.

33. Ganz SD. Replacing four mandibular incisors with an implant supported prosthesis. *Implant Soc.* 1993;4: 2–9.

34. Vassos DM, Petrik PK. The sinus lift procedure: an alternative to the maxillary subperiosteal implant. *Pract Periodont Aesth Dent.* 1992;4:14–19.

35. Judy KWM. Oral implantology case reports. *NYS Dent J.* 1986;52:24–26.

36. Wagner JR. A 3½-year clinical evaluation of resorbable hydroxylapatite OsteoGen (HA Resorb) used for sinus lift augmentations in conjunction with the insertion of endosseous implants. *J Oral Implantol.* 1991;17:152–164.

37. Wagner JR. A clinical and histological case study using resorbable hydroxylapatite for the repair of osseous defects prior to endosseous implant surgery. *J Oral Implantol.* 1989;15:186–192.

38. LeGeros RZ. Calcium phosphates in oral biology and medicine. In: Myers HM, ed. *Monographs in Oral Science.* New York: Karger Press; 1991: 15.

39. Fang Y, Agrawal DK, Roy DM. Thermal stability of synthetic hydroxylapatite. In: Brown PW, Constantz B, eds. *Hydroxylapatite and Related Materials.* CRC Press: Boca Raton, Fla: 1994:269–282.

40. Brown WE, Eidelman N, Tomazic B. Octacalcium phosphate as a precursor in biomineral formation. *Adv Dent Res.* 1987;1:306–313.

41. Urist MR, Dowell TA. The newly deposited mineral in cartilage and bone matrix. *Clin Orthopaed Rel Res.* 1967;50:291–308.

42. Bonar LC, Roufosse AH, Sabine WK, Grynpas MD, Glimcher MJ. X-ray diffraction studies of the crystallinity of bone mineral in newly synthesized and density fractionated bone. *Calcif Tissue Int.* 1983;35:202–209.

43. Roberts JE, Bonar LC, Griffin RG, Glimcher MJ. Characterization of very young mineral phases of bone by solid state phosphorus magic angle sample spinning nuclear magnetic resonance and x-ray diffraction. *Calcif Tissue Int.* 1992;50:42–48.

44. Lee DD, Landis WJ, Glimcher MJ. The solid, calcium-phosphate mineral phases in embryonic chick bone characterized by high-voltage electron diffraction. *J Bone Min Res.* 1986;1:425–432.

45. Roberts WE, Turley PK, Brezniak N, Fielder PJ. Bone physiology and metabolism. *Calif Dent Assoc J.* 1987;15:54–61.

46. Roberts WE. Bone tissue interface. *J Dent Educ.* 1988;52:804–809.

47. Brunski JB. Biomechanical factors affecting the bone-dental implant interface. *Clin Mat.* 1992;10:153–201.

48. Spivak JM, Ricci JL, Blumenthal NC, Alexander H. A new canine model to evaluate the biological response of intramedullary bone to implant materials and surfaces. *J Biomed Mat Res.* 1990;24:1121–1149.